ADVANCED FUNCTIONAL MATERIALS

Supporting Information

for *Adv. Funct. Mater.,* DOI: 10.1002/adfm.201910172

Plasmonic-Assisted Graphene Oxide Films with Enhanced Photothermal Actuation for Soft Robots

*Yuanyuan Yang, Yanting Liu, and Yajing Shen**

Supporting Information

Plasmonic-assisted Graphene Oxide Films with Enhanced Photothermal Actuation for Soft Robots

Yuanyuan Yang,[1,#] *Yanting Liu,*[1,#] *and Yajing Shen*[1,2,*]
[1] Department of Biomedical Engineering, City University of Hong Kong, 999077 Hong Kong SAR, China
[2] CityU Shen Zhen Research Institute, Shenzhen, 518000, China
[#] Equal contribution to this study
*E-mail: yajishen@cityu.edu.hk

Preparation of GO, rGO, rGO-PDA and GO-PDA solutions: GO was prepared using purified graphite according to the Hummers' method. Afterward, the GO solution was washed for several times to remove the residual ions, which was then centrifugated and then dispersed in distilled water. With ultrasonic treatment, the GO solution was collected at the concentration of 1 mg ml^{-1}. The rGO solution was obtained by a chemical reduction of the GO solution with HI solution (57 wt%) for 30 min. The resulted solution was washed and purified for several times to get the rGO solution. To obtain rGO-PDA solution, 15 ml Tris buffer (Ph = 8.5) was mixed with 15 ml 2mg/ml GO solution. Then 60 mg DA was added and dispersed by sonication for 10 min in ice bath. The mixed solution was sirred at 60 °C for 24 h. Afterward, solution was washed several times to remove free PDA particles. To obtain the GO-PDA solution, 7 mg DA was mixed with 15 ml 2mg/ml GO solution and sonicated for 1 h. Following, the PH value of the mixed solution was adjusted to 8.5 using 1 mol/ml Tris solution. The resulted solution was then stirred for 12 h at 45 °C to get the GO-PDA solution.

Fabrication of GO/PDMS, rGO/PDMS, rGO-PDA/PDMS and GO-PDA/PDMS film: PDMS was prepared at a 10:1 weight ratio (base: curing agent) and under spinning coating on the glass substrate at the speed of 500 rpm for 15 s and 900 rpm for 30 s. Then, PDMS was cured at the temperature of 75 °C for 2 h and transferred to the dish (r= 27 mm). After plasma treatment on the PDMS surface, 5 ml of GO, rGO, rGO-PDA and GO-PDA solutions were poured into dish and dried at 75 °C for 5 h seperately. This operation was repeated two more times, and the GO/PDMS, rGO/PDMS, rGO-PDA/PDMS and GO-PDA/PDMS film bilayer films were obtained after peeling off.

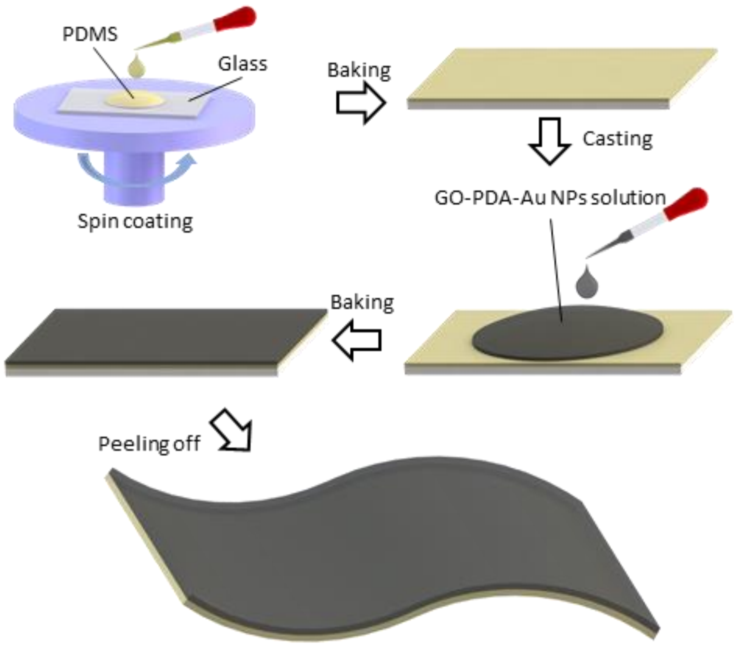

Figure S1. Fabrication of bilayer film. The GO-PDA-Au NPs solution is cast on the surface of PDMS and baked. The bilayer film is obtained by peeling off.

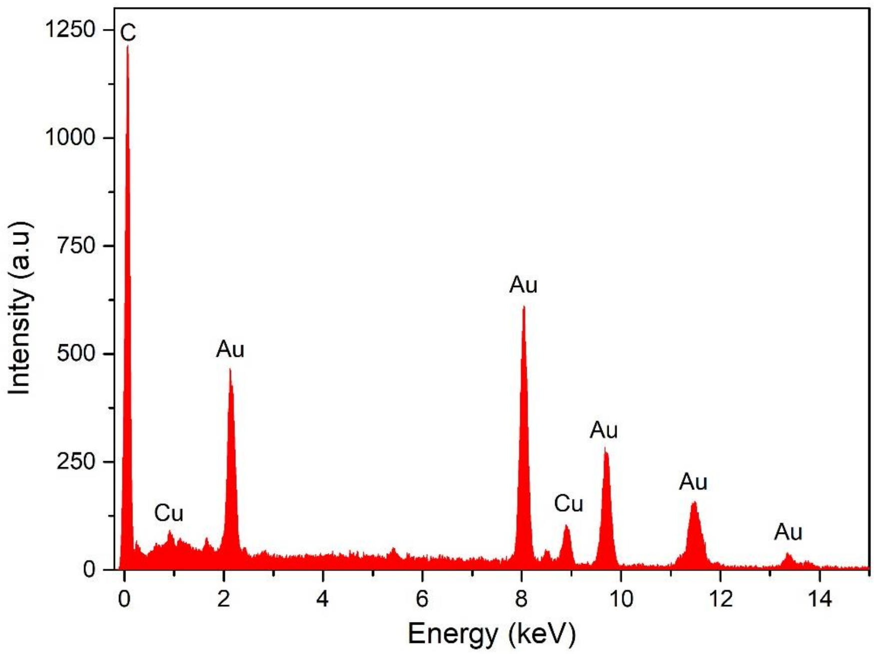

Figure S2. Energy dispersive spectro indicates that there are two constituent elements Au and C in the composite.

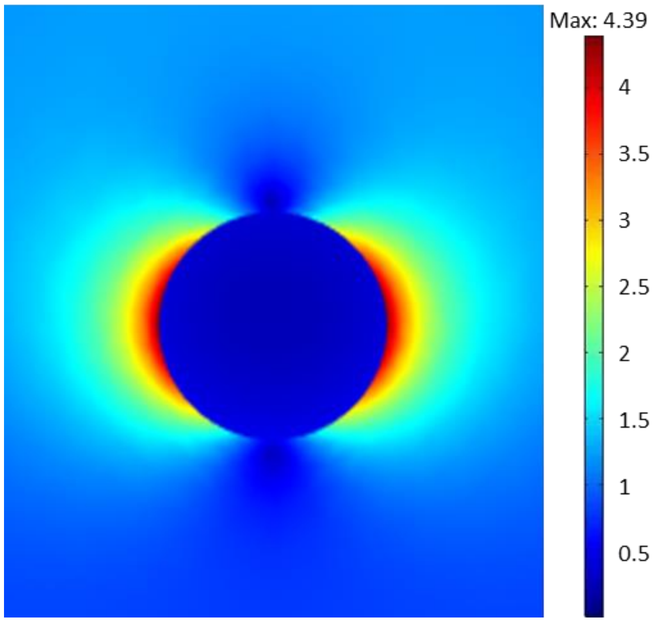

Figure S3. COMSOL simulation of electric field enhancement. The simulation of a single Au NPs (85 nm) shows an enhancement of the electric field on the nanosphere surface by the 808 nm wavelength incident light.

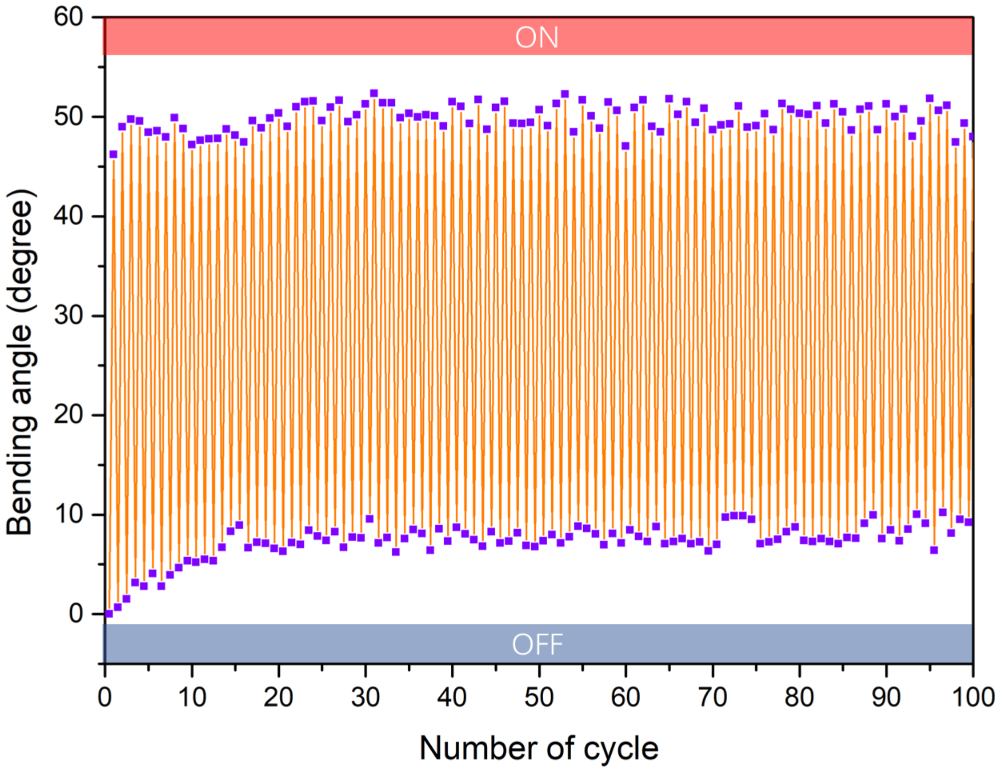

Figure S4. Bending angle of GO-PDA-Au NPs/PDMS composite film over 100 cycles of light actuating (laser power: 3 W/cm^2). Between different cycles, the bending angle differs with errors but with stable bending-recovery performance and good reversibility.

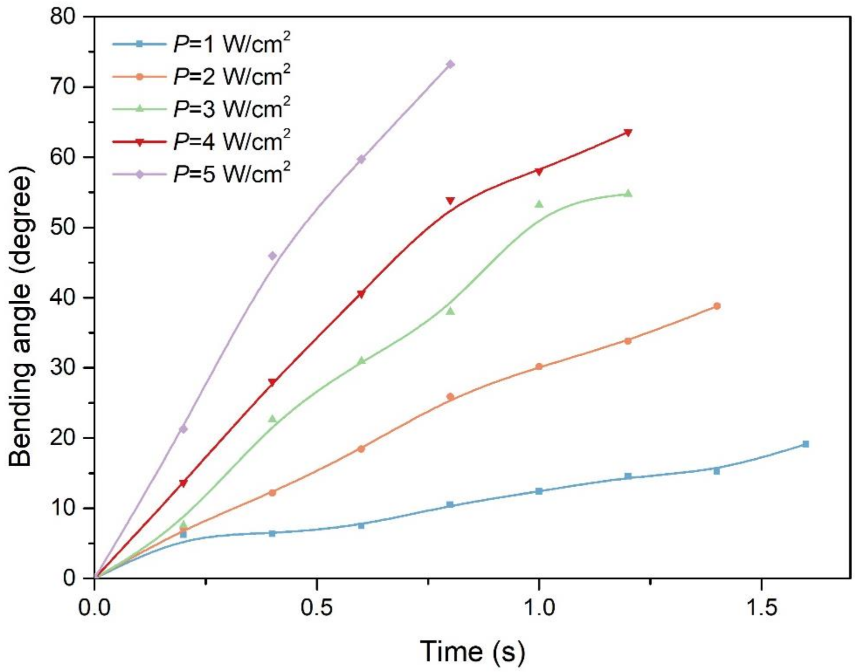

Figure S5. Bending angle of GO-PDA-Au NPs/PDMS composite film under different light powers according to time. With high laser power, the bending angle increases and the corresponding response time is shortened.

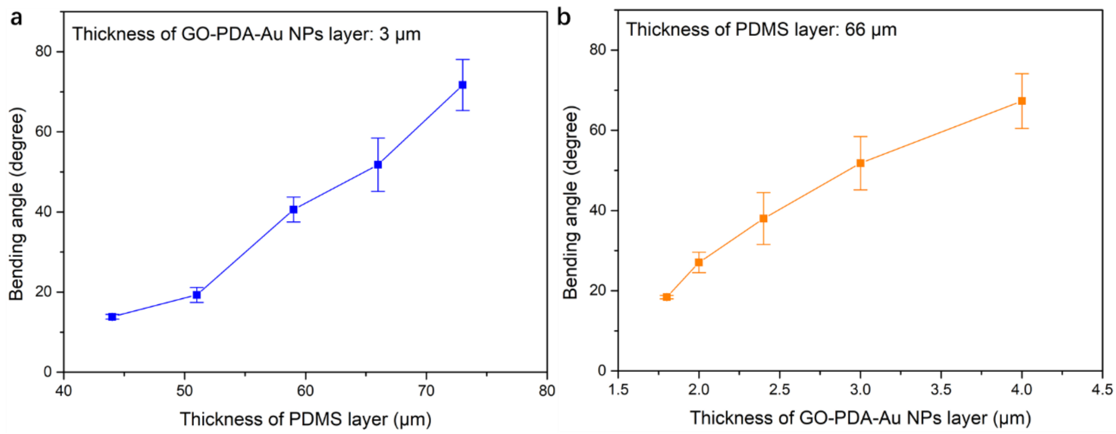

Figure S6. Bending angle of GO-PDA-Au NPs/PDMS composite film with different thicknesses of separate layer. a) With the same thickness of the GO-PDA-Au NPs layer (3 μm), the bending angle increases along with the thickness of the PDMS layer. b) With the same thickness of the PDMS layer (66 μm), the bending angle increases along with thickness of the GO-PDA-Au NPs layer.

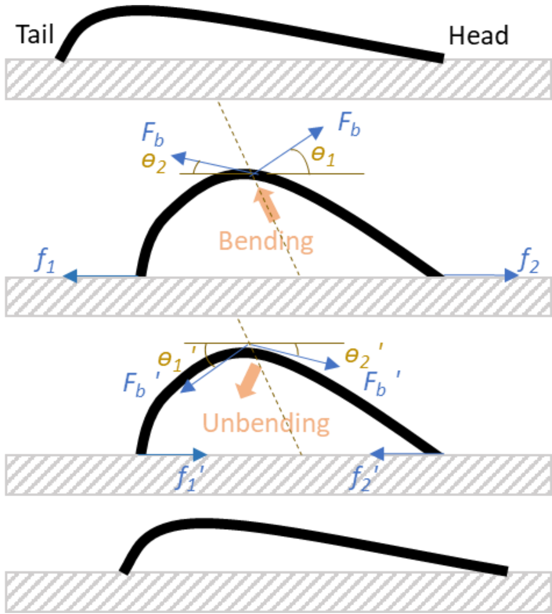

Figure S7. Locomotion mechanism of rectangular soft robot.

The robot is designed with an irregular angle as shown in Figure S7. When NIR light is applied, the whole robot body bends upward. The robot body can be divided into the right part (head) and the left part (tail). The friction force for tail f_1 and head f_2 is

$$f_1 = \mu(\frac{1}{2}mg - F_b \sin\theta_1) \tag{1}$$

$$f_2 = \mu(\frac{1}{2}mg - F_b \sin\theta_2) \tag{2}$$

Where the μ is the friction coefficient, m is the mass of robot, g is the gravitational acceleration, F_b is the bending force.

$$\theta_1 > \theta_2 \tag{3}$$

Thus

$$f_1 < f_2 \tag{4}$$

The tail moves forward.

After withdrawing the NIR light, the robot's body unbends downward. In this moment, the friction force for tail f_1' and head f_2' is

$$f_1' = \mu(\frac{1}{2}mg + F_{ub} \sin\theta_1') \tag{5}$$

$$f_2' = \mu(\frac{1}{2}mg + F_{ub} \sin\theta_2') \tag{6}$$

$$\theta_1' > \theta_2' \tag{7}$$

Where F_{ub} is the unbending force. Thus

$$f_1' > f_2' \tag{8}$$

The head moves forward. By repeating such cycles, the robot moves forward periodically.

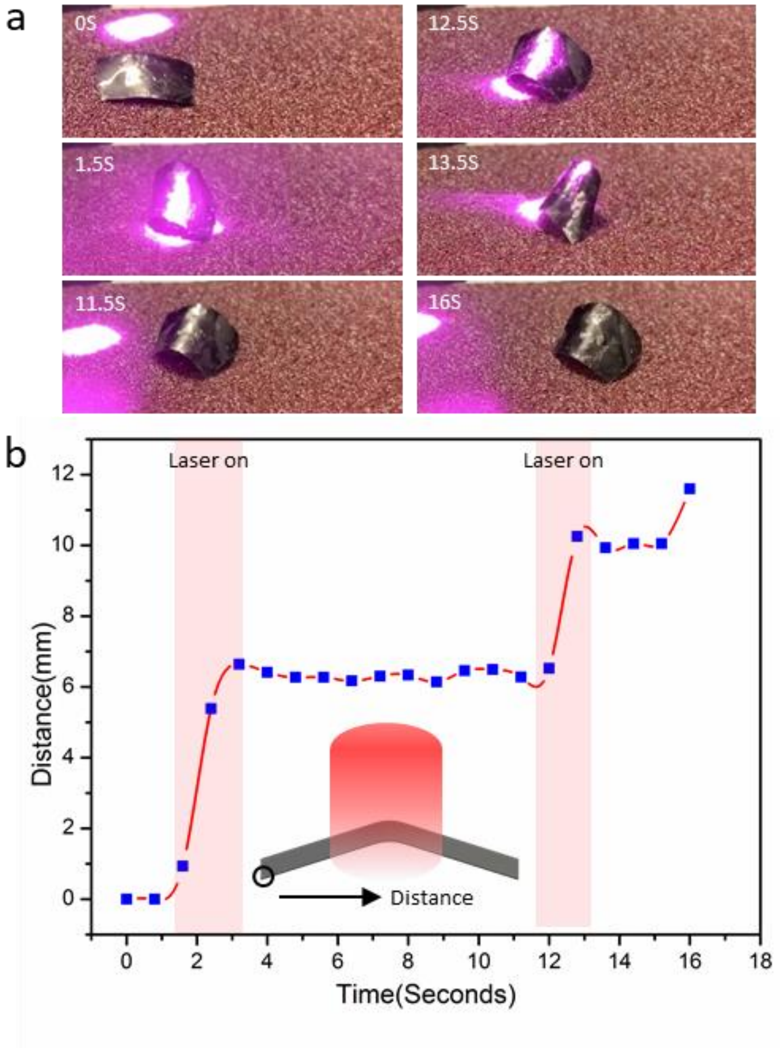

Figure S8. Forward motion of irregular quadrangle robot on a rough surface. a) Digital images of forward motion by contraction and extraction. b) Moving distance according to time during two locomotion cycles.

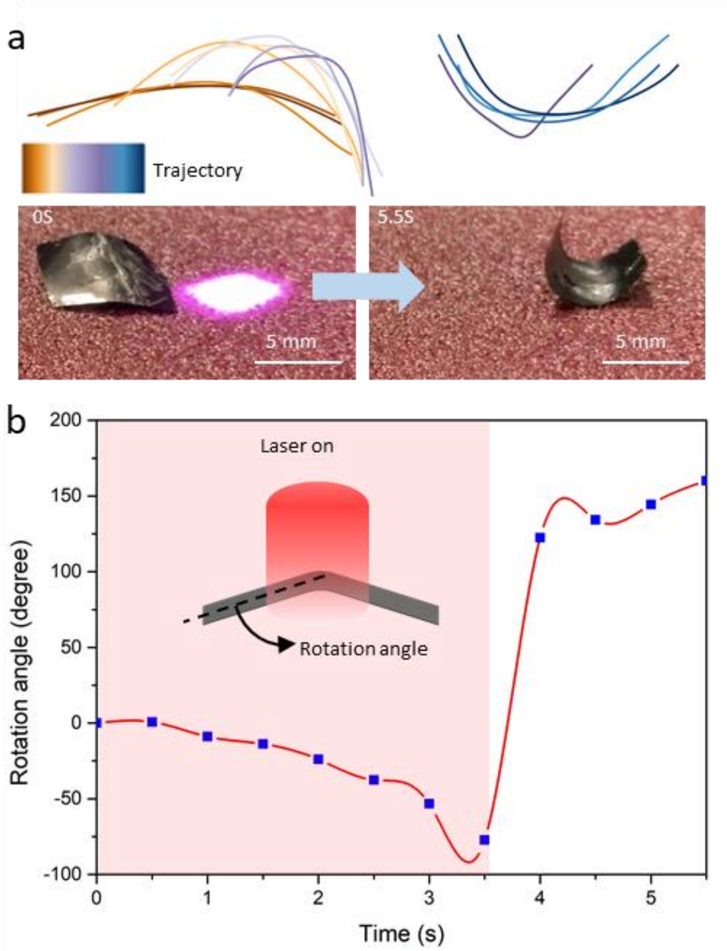

Figure S9. Rolling motion of irregular quadrangle robot on a rough surface. a) Digital images of rolling motion. The bending of the robot body leads to an unbalanced state, so the robot rolls over. b) Rotation angle of the robot during rolling.

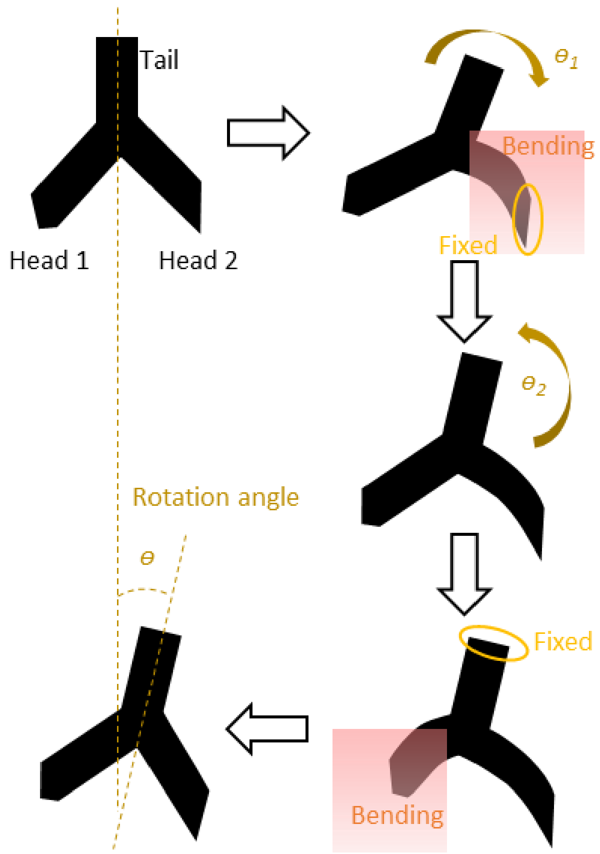

Figure S10. Steering motion mechanism of triple-legged robot.

The shapes of heads 1 and 2 are shown in Figure S10. In the beginning, NIR light is focused on head 2 resulting in its bending. As head 2 is in surface contact with the ground, its friction force is higher than those of head 1 and tail. Thus, head 2 is fixed while head 1 and tail rotate with an angle θ_1. After withdrawing the light, head 2 unbends so that head 1 and tail rotate back with angle θ_2. Before they rotate to their original place, light is focused on head 1 that it bends. The angles of heads 1 and 2 are the same for a moment during bending and unbending process separately. At this moment, the tail is in surface contact with the ground that it is fixed. After removing the light, the two heads move according to the tail position. The bending angle of the whole process θ would be

$$\theta=\theta_1-\theta_2 \tag{9}$$

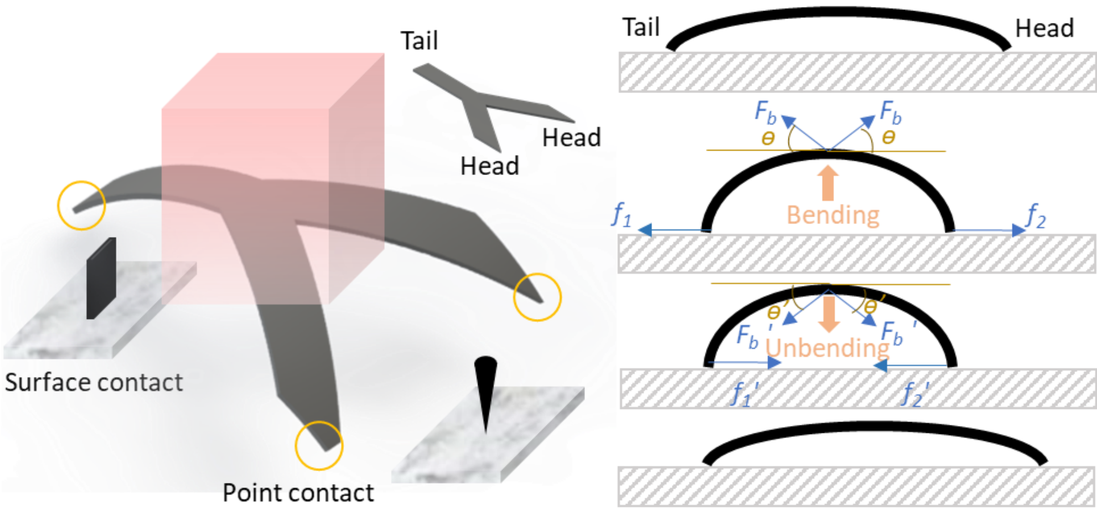

Figure S11. Linear motion mechanism of triple-legged robot.

During the locomotion of the triple-legged robot, the tail is in surface contact with the ground, whereas the two heads are in point contact with the ground. As a result, the friction coefficient of the tail and head μ_1 and μ_2

$$\mu_1 > \mu_2 \tag{10}$$

$$F_b \cos\theta > \mu_1(\frac{1}{2}mg - F_b \sin\theta) > \mu_2(\frac{1}{2}mg - F_b \sin\theta) \tag{11}$$

Where m is the mass of robot, g is the gravitational acceleration, F_b is the bending force. The tail moves forward, and heads move back that whole robot body contracts. During the unbending process,

$$\mu_1(\frac{1}{2}mg - F_{ub} \sin\theta') > F_{ub} \cos\theta' > \mu_2(\frac{1}{2}mg - F_{ub} \sin\theta') \tag{12}$$

F_b is the unbending force. Consequently, the tail keeps still while the heads stretch out. After one cycle of locomotion, the whole robot body moves forward.